Near single-crystal electrical properties of polycrystalline HgI_2 produced by physical vapor deposition

A. Zuck,[(a)]* M. Schieber, [(a)]** O. Khakhan, [(a)] Z. Burshtein [(b)]***

School of Applied Science and Technology, The Hebrew University of Jerusalem, Jerusalem 91904, Israel

[a] Also with Real Time Radiography, Jerusalem Technology Park, Jerusalem 91487, Israel
[b] Materials Engineering Department, Ben-Gurion University of the Negev, P.O.B. 653, Beer-Sheva 84105, Israel

Abstract - Transient charge transport (TCT) measurements were used to evaluate the electrical conduction properties of polycrystalline HgI_2 prepared by physical vapor deposition (PVD). The mobility μ, trapping time τ, and surface recombination velocity s of electrons or holes were determined by analyses of transient voltages developed across the sample in response to a drift of the corresponding charge carriers created by alpha particle absorption near one of the electrodes. Typical electron-, and hole mobilities were $\mu_n = 88\ \text{cm}^2/\text{V}\cdot\text{s}$ and $\mu_p = 4.1\ \text{cm}^2/\text{V}\cdot\text{s}$, respectively; Trapping times were $\tau_n \gtrsim 16\ \mu\text{s}$ and $\tau_p \lesssim 3.5\ \mu\text{s}$, and surface recombination velocities $s_n \cong 1.4\times10^5\ \text{cm/s}$ and $s_p \cong 3.7\times10^3\ \text{cm/s}$. All parameters depend to a large extent on the material deposition technology. The effect of carriers being first generated in near-surface traps and then gradually released is observed. It is similar, somewhat more pronounced than that observed for a single-crystal by using the same method [1].

Index Terms - Mercuric iodide, polycrystalline mercuric iodide, transient charge transport (TCT), mobility, lifetime, trap emission time, surface recombination.

I. INTRODUCTION

Transient charge transport (TCT) measurement is recognized since the 1970's [2] as a reliable method for evaluating basic electrical properties such as mobility μ and trapping time τ in high-resistivity semi-conductors. Roth et al [3,4] adopted the method to study HgI_2 and CdSe semiconductor radiation detectors in 1987.

Summaries of μ and τ values for HgI_2 single-crystal detectors measured by different methods are provided in various publications [5]. Some of the measuring methods are based on Hecht's equation for charge collection as a function of bias. Sometimes nuclear spectroscopy is utilized, for example by observation of the photo-peak energy-shift as a function of bias [5]. In a recent study, a simulation of the $\mu\tau$ product to fit the experimental spectral width of ^{137}Cs emission spectrum (660 keV gamma ray) was used [6]. In general, the electron effective $\mu\tau$-product for the single crystal [5] is of the order of $\sim 10^{-4}\ \mathrm{cm}^2/\mathrm{V}\cdot\mathrm{s}$.

Thick film Polycrystalline HgI_2 is most promising as a direct photo-conduction converter in x-ray digital radiography. It exhibits the highest x-ray sensitivity among the known polycrystalline or amorphous materials [7]. Physical vapor deposition (PVD) has been used [8] for preparation. Description of preparation methods, characterization of detection capability, and first imaging results, were recently published [9]. The sensitivity and charge transport properties of PVD polycrystalline x-ray detectors are somewhat inferior to those of the single crystal [10]. Grain boundaries in the polycrystalline material are expected to be electrically active [11], for example by creating trapping levels within the forbidden gap. Their disturbance to charge collection includes the introduction of potential barriers between neighboring grains [12,13], and of electron-hole recombination and trapping centers. All efforts to improve the crystalline microstructure and material purity are aimed at enhancement of the charge collection efficiency.

The present work adopts the method of transient charge transport measurement to assess the quality of polycrystalline mercuric iodide layers prepared for x-ray detectors. The method was first attempted on a single crystal by the same authors,

revealing, however, a new effect: the delayed emission of carriers, initially generated in near-surface traps. A similar effect was obtained for the polycrystalline layers.

II. THEORETICAL BACKGROUND

Ionizing radiation absorption in an insulating, photo-conducting detector is followed by the generation of free charge carriers. The charge collection efficiency is defined as $\eta \equiv Q/Q_0$, where Q is the actual charge collected by the electrodes under an applied voltage, and Q_0 is the charge that would have been collected had all carrier trapping and recombination processes been avoided. When all carriers are generated near one electrode, the collection efficiency η is given by Hecht's equation [14]

$$\eta = \frac{\mu \mathbf{E} \tau}{L}\left[1 - \mathbf{exp}(-L/\mu \mathbf{E} \tau)\right] \quad , \quad (1)$$

where L is the detector thickness, $\mathbf{E}$ the electric field, μ the mobility of the carrier type swept from the electrode into the material bulk (holes for a positive polarity, electrons for a negative one), and τ is the bulk trapping or recombination time of the same-type carrier. For a constant electric field, the charge collection efficiency increases with both mobility and trapping time. Thus the product $\mu\tau$ serves as a figure of merit for detector quality. Experimentally, the product $\mu\tau$ may be extracted from the measured field of half-maximum charge-collection $\mathbf{E}_{hmc}$ in the collected charge versus electric field plot. It is then given by $\mu\tau = 0.63L/\mathbf{E}_{hmc}$. Obviously, when the opposite polarity is applied to the irradiated electrode, the corresponding carrier mobility and its bulk trapping time should be inserted in Eq. (1), yielding a different $\mu\tau$ product.

If carrier generation takes place throughout the detector bulk, summation over collection efficiencies of both carrier-type distributions should be made, taking account of the actual distance traveled by each carrier. Whichever generation distribution is selected, the outcome is always a function resembling the nature of Eq. (1); namely, the collection efficiency is an increasing function of the electric field, starting at zero and saturating at unity for higher fields. For that reason, an "effective $\mu\tau$ product" is defined by using the same expression: $(\mu\tau)_{eff} = 0.63L/\mathbf{E}_{hmc}$.

In 1983, Levi et al [15] pointed out that whenever carriers are generated sufficiently close to the surface, surface recombination of charge carriers sets in, in addition to bulk trapping. Hecht's equation for a near-electrode (near surface) carrier generation must then be corrected to take account of surface recombination:

$$\eta = \frac{1}{1 + s/\mu \mathbf{E}} \cdot \frac{\mu \mathbf{E} \tau}{L} \left[1 - \mathbf{exp}(-L/\mu \mathbf{E} \tau)\right] \quad , \qquad (2)$$

where s is the surface recombination velocity of the corresponding charge carrier. The electric field at half-maximum collection is accordingly approximated by

$$\mathbf{E}_{hmc} \cong \frac{s}{\mu} + 0.63 \frac{L}{\mu \tau} \quad . \qquad (3)$$

For $s >> L/\tau$, saturation of charge collection is governed by surface recombination. Thus, an "effective $\mu\tau$ product" obtained under near-surface generation may not, and should not be generalized to cases of uniform bulk charge-carrier generation.

Measurements of transient charge transport (TCT) in photo-conductors allow the simultaneous determination of mobility and trapping-times. The method is based on tracing the transient voltage waveforms (voltage signals, hereafter) created across a biased detector by short carrier-generation events. The latter may be achieved by short, strongly absorbed laser pulses, short, low energy electron beam pulses, or ionizing radiation quanta (alpha) [3,4]. The use of a positive or a negative polarity to the irradiated electrode allows separate analyses of hole- and electron transport kinetics, respectively. Provided that carrier de-trapping times are very long compared to their transit time $t_t = L/\mu \mathbf{E}$ across the sample, the voltage signal $\delta V(t)$ would be given by

$$\delta V(t) = \begin{cases} 0 & t < 0 \\ \dfrac{Q_0 L}{\varepsilon_r \varepsilon_0 A} \cdot \dfrac{1}{1 + s/\mu \mathbf{E}} \cdot \dfrac{\tau}{t_t} \left[1 - \mathbf{exp}(-t/\tau)\right] & 0 < t < t_t \\ \dfrac{Q_0 L}{\varepsilon_r \varepsilon_0 A} \cdot \dfrac{1}{1 + s/\mu \mathbf{E}} \cdot \dfrac{\tau}{t_t} \left[1 - \mathbf{exp}(-t_t/\tau)\right] & t > t_t \end{cases} \quad , \qquad (4)$$

where ε_0 is the permittivity of free space, ε_r is the relative dielectric constant of the detector material, and A is the detector area. The voltage signal is obviously proportional to the collected charge. The charge-carrier generation event takes place at $t = 0$. Since after the transit time the signal remains constant, the transit time is sharply

defined, allowing a simple determination of the mobility. The trapping time can be obtained independently from the waveform shape analysis. Inclusion of the surface recombination effect in Eq. (4) allows the determination of the surface recombination velocity as well. In principle, measurements of the transient current rather than of transient voltage provide a better resolution of all parameters. However, excitation of excessively more charge carriers would be needed in order to resolve current signals; in a series of measurements, this often causes the development of polarization due to trapped charge in the sample bulk.

Experimental measurements in single crystals which we carried out recently [1] indicated, that under certain cases, a part of the charge carriers are generated in surface shallow traps, and are later emitted on a different time scale. We assume that the appearance of free charge Q_f near the electrode satisfies

$$dQ_f(t) = \begin{cases} fQ_0 & t = 0 \\ \dfrac{(1-f)}{\tau_{em}} Q_0 \, \mathbf{exp}(-t/\tau_{em})dt & t > 0 \end{cases} , \qquad (5)$$

where f is the fraction of promptly-generated free carriers, and τ_{em} is the characteristic emission-time of the promptly-generated surface-trapped carriers. The actual voltage signal across the sample $\delta V_{act}(t)$ is given in terms of the simple expressions of Eq. (4) as a convolution

$$\delta V_{act}(t) = f \cdot \delta V(t) + \frac{(1-f)}{\tau_{em}} \int_0^t \delta V(t-t') \mathbf{exp}(-t'/\tau_{em}) dt' \quad . \qquad (6)$$

To demonstrate the effect of delayed surface-carrier emission, in Fig. 1 we show numerical computation results for actual voltage signal (collected charge) vs. time traces expected under different relations among t_t, τ, and τ_{em}, for $f = 0.5$. Traces for very long emission times are given in Fig. 1(a). Apart from a factor of f lowering of the total charge collected, the delayed carrier emission has no effect on the traces. In Fig. 1(b), we show traces expected for a relatively short emission time, $\tau_{em} = t_t$. The transit time is best resolved when it is shorter than both τ and τ_{em}. It is practically impossible to resolve when it is equal to-, or longer than τ or τ_{em}. In the special case $f << 1$, the trace-shape reflects the shorter between τ and τ_{em} under two extreme conditions: when $t_t << \tau, \tau_{em}$ or when $t_t >> \tau, \tau_{em}$. For example, suppose that

$\tau << \tau_{em}$; then, the point in time where the trace reaches 95% of its maximal value, $t_{0.95}$, is approximately 3τ. If on the other hand $\tau_{em} << \tau$, then $t_{0.95}$ is approximately $3\tau_{em}$. We refer later to $t_{0.95}$ as an "effective transit-time".

While the trapping- and emission times are expected to be independent of voltage across the sample, the transit time is strictly inversely proportional to it. Thus, changing of voltage bias across the sample allows t_t, τ or τ_{em} to be extracted from characteristic features of the voltage-signal versus time traces.

III. EXPERIMENTAL

Two polycrystalline mercuric iodide (poly-HgI_2) film detectors, 220-, and 240 micrometers thick, were prepared by physical vapor deposition (PVD) [7]. The film detectors were manufactured by Real-Time Radiography Ltd., Jerusalem, Israel (RTR), and belonged to two different batches marked G3 and G4, respectively. We present results on a sample from the G4 batch only. The films are deposited on indium-tin-oxide (ITO)-coated glass substrates. A thin (~ 500 nm), semitransparent layer of colloidal graphite (Aquadag by Acheson) was painted as a front electrode, approximately $10\ mm^2$ in area. A ^{241}Am alpha-particle source (5.5 MeV) was used to induce near-surface carrier-generation events. A collimator of approximately $1\ mm^2$ in area in front of the detector served to limit the alpha incidence rate to less than $\sim 1{,}000$ per second. The alpha source was mounted at approximately 0.5 mm distance from the front detector electrode.

The set-up and typical electrical scheme for the transient voltage measurement is shown in Fig. 2. The high voltage across the detector was provided by a 240A type KEITHLEY power supply. The detector was shunted with a series resistance of the order of $100 - 1{,}000\ M\Omega$, depending on the long time-scale needed for measurement. Voltage signals across this resistor follow the alpha particle absorption. They are fed into the input of a source-follower preamplifier of approximately unity amplification, which serves for impedance matching, then into a Tektronix TDS210 digital oscilloscope. The time resolution exhibited by the circuitry at point B was approximately $0.05\ \mu s$. For low voltage bias, further pre-amplification was required,

however at the cost of reduced time resolution (point A in Fig. 2). Pulse shapes were digitally recorded by a desktop personal computer, and displayed on the screen with the aid of WAVE-STAR software.

IV. RESULTS AND DISCUSSION

A. Transit-time and mobility

Voltage transient response of each detector to excitation by $5.5\ \mathrm{MeV}$ alpha particles was recorded as a function of bias for both positive and negative polarities. Figure 3 shows two voltage-versus-time waveforms obtained by irradiating the negative electrode of a polycrystalline detector biased at $-80\ \mathrm{V}$, and the positive electrode of the same detector biased at $+200\ \mathrm{V}$, respectively. Alpha particle absorption causes a burst of charge-carrier generation. The collected charge rises afterwards, and eventually it saturates. The transit time t_t is resolved by the sharp turn of the voltage to saturation, indicating that neither strong trapping nor considerable delayed de-trapping occurred in these cases (Fig. 3). The transit time for each case of Fig. 3 is indicated in the figure.

The transit time for each carrier is given by

$$t_t = \frac{L^2}{\mu V} = \left(\frac{L^2}{\mu}\right) \cdot \frac{1}{V} \quad . \qquad (7)$$

The transit time for the measurements of Fig. 3 and for other voltages is shown for each polarity in Figs. 4(a) and 4(b) as function of the inverse voltage. The proportionality of the transit time to the inverse voltage expected by Eq. (7) is verified. The electron and hole mobilities extracted from the experimental slopes are $\mu_n = (87 \pm 3)\ \mathrm{cm^2/V \cdot s}$ and $\mu_p = (4.1 \pm 0.15)\ \mathrm{cm^2/V \cdot s}$, respectively. Similar measurements by Roth and others [3,4] on HgI_2 single crystal yielded $\mu_n = 97\ \mathrm{cm^2/V \cdot s}$, and $\mu_p = 4\ \mathrm{cm^2/V \cdot s}$.

The near-similarity of the PVD polycrystalline HgI_2 electrical properties to that of a single crystal is quite surprising, yet may be accounted for by the unique nature of the polycrystallinity achieved. High-mobility samples exhibit a columnar structure. The columns are highly oriented in the (001) direction (c-axis), which is normal to the

layer surface. [15]. Different average column length is obtained for different variations in fabrication procedures. In fact, a most important prerequisite for obtaining a non-porous, dense, sufficiently thick HgI_2 layer, is to activate the preferential growth along the c-axis, namely to have the c-axis of the grains preferentially oriented perpendicular to the substrate plane. A charge-carrier may thus drift between two column edges without encountering excess trapping or recombination at grain boundaries. If the material is sufficiently pure, and the typical grain is sufficiently long approaching the sample thickness, the PVD layer may exhibit similar electrical properties as the single crystal.

B. Carrier lifetime and trap emission time

Consider first the effective transit time $t_{0.95}$ if no delayed free-charge generation occurs. If it is proportional to the inverse voltage V^{-1}, it may then be interpreted as the true transit time (Fig. 1(a); Eq. (6)). If it is shorter than the calculated transit-time, and independent of inverse voltage, it could then be interpreted as three-times the trapping time:- 3τ.

In Fig. 5 we show results obtained for the single crystal at both negative and positive polarities. For low inverse voltages (high voltages), the definition of $t_{0.95}$ was sharp, repeatable among different traces, and linearly proportional to the inverse voltage. It is virtually identical with the corresponding transit-time results of figures 4(a) and 4(b), yielding the same mobility. Note that the inverse-voltage scales in Fig. 5 (especially 5(a)) are too coarse to allow clear resolution of the different points shared with Fig. 4(a). For higher inverse voltages, the $t_{0.95}$ results show a large scatter; yet on the average they also show a regular behavior. The dashed curves in both Figs. 5(a) and 5(b) are empirical, and are aimed at guiding the eye towards that regular behavior. The dash-dotted lines are extrapolations of the transit time.

In the intermediate range, $t_{0.95}$ increases with the inverse voltage. For electrons (5(a)) it is longer than the calculated transit time. Then it saturates to a constant value, $\sim 50\ \mu s$, which is substantially longer than the extrapolated transit time for the inverse-voltage range studied. For holes (5(b)), it is initially longer than the calculated transit

time. Then it also saturates to a constant value, $\sim 11\ \mu s$, at higher inverse voltages, which is however shorter than the extrapolated transit time for those voltages.

We interpret the $t_{0.95}$ times in the intermediate inverse voltage region as reflection of delayed charge carrier emission time τ_{em} out of shallow near-surface traps for both electrons and holes (Eq. (4) and Fig. 1). A clear demonstration of this effect is provided in Fig. 6 below. In Fig. 5, this characteristic emission time appears to grow longer with inverse voltage both for holes and electrons. In other words, τ_{em} becomes shorter with increasing electric field (namely $\tau_{em} = \tau_{em}(\mathbf{E})$). The saturated $t_{0.95}$ provides an upper limit estimate for either $3\tau_{em}(\mathbf{E}=0)$ or 3τ. Observation of the voltage signal traces shown in Fig. 6 indicates that for electrons $\tau \gtrsim \tau_{em}$, while for holes $\tau \lesssim \tau_{em}$. Thus for electrons, $\tau_n \gtrsim 16\ \mu s$ and $\tau_{em}^{(n)}(\mathbf{E}=0) \lesssim 16\ \mu s$. For holes, $\tau_p \lesssim 3.5\ \mu s$ and $\tau_{em}^{(p)}(\mathbf{E}=0) \gtrsim 3.5\ \mu s$. The "p" or "n" sub-/superscripts indicate relation to holes or electrons, respectively.

We assign the very large scatter in $t_{0.95}$ to statistical variations in the lateral position on the surface where alpha particles enter, variations in their remaining energy after traversing the air-gap and contact material, and variations in the local density of surface traps. Further study is required to fully understand the role of each factor mentioned, which we intend to perform in the near future. We also intend to study of the electric field dependence of τ_{em}.

A direct demonstration of the delayed carrier emission in intermediate inverse voltages is provided in Fig. 6. The voltage signal trace for electron collection in Fig. 6(a) exhibits a considerable growth past the calculated transit time. One observes no turning indicative of τ (lower traces in Figs. 1(a) and 1(b)). Thus we conclude that $\tau_n \gtrsim \tau_{em}^{(n)}$. In Fig. 6(b), the initial fast rise resembles the lower trace in Fig. 1(b). Thus we conclude that $\tau_p \lesssim \tau_{em}^{(p)}$.

C. Charge collection and surface recombination velocity

The charge collection against the applied electric field (the "Hecht" curve) is shown in Figs. 7(a) and 7(b) for a negative and a positive polarity, respectively. The curves saturate at $100\ \text{fC}$ for electrons, and $35\ \text{fC}$ for holes. The free charge generated in

alpha particle absorption would be given by $Q_0 = qE_\alpha/w$, where $w = 4.2$ eV is the known average electron-hole generation energy in HgI_2, q is the electronic charge, $E_\alpha = 5.5$ MeV is the alpha particle energy. Thus we get $Q_0 \cong 200$ fC. We assign the reduced charge generation partly to energy loss by the alpha particle on passing through the contact. Still, the maximal collected charge is considerably different between electrons and holes (100 - as compared to 35 fC, respectively). For 100% free-carrier generation, no such difference should occur. This result is however consistent with the existence of different near-surface deep carrier traps for electrons and holes, which exhibit long emission times on the measurement time scale. In other words, different carriers exhibit both different free-carrier generation fraction f, and different trapped carrier emission time τ_{em} at the high voltage (Eq. (3)). Each electric field of half-maximum charge collection is readily obtained: 0.18×10^4 V/cm for electrons, and 0.19×10^4 V/cm for holes.

Given the estimated electron and hole trapping time, and the measured mobility and field of half-maximum collection, each carrier surface recombination velocity is readily calculated using Eq. (3). One obtains $s_n \cong (1.55 \pm 0.1) \times 10^5$ cm/s, and $s_p \lesssim (3.8 \pm 0.4) \times 10^3$ cm/s. The electron surface recombination velocity is an order of magnitude larger than typical best values obtained for HgI_2 detectors. The hole surface recombination velocity appears a factor of three smaller than ever reported [15,17]. We suspect that the absence of a top electrode passivation layer, (thin Humiseal) in the present study is responsible for the enhanced electron surface recombination velocity. It has already been established [17], that exposure to free air affects the surface electrical properties.

V. CONCLUSIONS AND SUMMARY

Transient charge transport (TCT) measurements were used to evaluate the electrical conduction properties of polycrystalline HgI_2 prepared by physical vapor deposition. The mobility μ, trapping time τ, and surface recombination velocity s of electrons or holes were determined by analyses of transient voltages developed across the sample in response to a drift of the corresponding charge carriers created by alpha particle

absorption near one of the electrodes. The measurements revealed a new effect: the delayed release of carriers initially generated in near-surface traps. Current theoretical expressions were extended to include this effect, which may be characterized by the fraction of free-generated charge f and surface-trapped carrier emission time τ_{em} (Eqs. (5) and (6)). The theory allows the description of cases involving surface generation and recombination, drift, as well as bulk trapping.

Electron-, and hole mobilities in the polycrystalline HgI_2 depend on the film deposition technology. Mobilities measured for different samples vary between 65-, and $(87 \pm 3)\ cm^2/V \cdot s$ for electrons, and between 4.3-, and $(4.1 \pm 0.15)\ cm^2/V \cdot s$ for holes. These values are surprisingly close to those of a single crystal [1]. This apparently stems from the long-columnar polycrystalline structure and high purity of the layers. Bulk trapping-times and hole surface recombination velocities also appear of the same order of magnitude as in the single crystal. Electron surface recombination may most likely be reduced substantially by proper surface treatment and passivation. This puts the PVD-prepared HgI_2 layer as a favorable candidate material for gamma and x-ray detection.

We intend to further use the TCT method in obtaining comprehensive evaluations of electrical properties in polycrystalline HgI_2. We will put emphasis on understanding the origin and nature of the surface traps.

ACKNOWLEDGMENT

Participation of one of the authors, O. Kh., was made possible by a grant from the Shapira Foundation, Ministry of Immigrant Absorption, State of Israel.

REFERENCES

[1] A. Zuck, M. Schieber, O. Khakhan, and Z. Burshtein, "Delayed emission of surface-generated trapped carriers in transient charge transport of single-crystal and polycrystalline HgI_2," *Proc., SPIE in Hard X-ray and Gamma-Ray Detector Physics IV, conf. , Seatle, 2002*, in press.

[2] J. Martini, W. Mayer, and K. R. Zanio, "Drift Velocity and Trapping in Semiconductors - Transient Charge Technique," in *Applied Solid State Physics*, Vol. 3, pp. 181-243, 1972.

[3] M. Roth, A. Burger, J. Nissenbaum, and M. Schieber "Transient Charge Technique Investigation of HgI_2 and CdSe Nuclear Detectors," *IEEE Trans. Nucl. Sci*. vol. NS-34, pp. 465-469, 1987

[4] H. Hermon, M. Schieber, and M. Roth, "Study of trapping levels in doped HgI_2 radiation detectors," *Nucl. Instr. Meth. Phys. Res. A*, vol. 380, pp. 10-13, 1996.

[5] X. J. Bao , T.E. Schlesinger, R.B. James, "Electrical Properties of Mercuric Iodide," in *Semiconductors and semimetals* vol. 43, Ch. 4, Academic Press, San Diego, 1995.

[6] J. E. Baciak, Z. He, and R. P. Devito, "Electron trapping variations in single-crystal pixelated HgI_2 gamma-ray spectrometers," in *Nuclear Science Symposium Conference Record, 2001 IEEE* , vol.4, pp. 2335–2339, 2002

[7] M. Schieber, H. Hermon, A. Zuck, A. Vilensky, L. Melekhov, R. Shatunovsky, E. Meerson, Y. Saado, M. Lukach, E. Pinkhasy, S.E Ready, R.A Street, "Thick Films of X-ray Polycrystalline Mercuric Iodide Detectors," *J. Cryst. Growth,* vol. 225, pp. 118-123, 2001.

[8] M. Schieber, H. Hermon, A. Zuck, A. Vilnsky, L. Melekhov, R. Shantunovsky, E. Meerson, H. Saado, "Polycrystalline Mercuric Iodide Detectors," *Proc. Medical Applications of Penetrating Radiation,* SPIE vol. 3770, pp. 146-155, 1999.

[9] R. A. Street, S.E. Ready, J.T. Rahn, M. Mulato, K. Shah, P. Bennet, P. Mei, J. Lu, R. Apte, J. Ho, K. Van Schuylenbergh, F. Lemmi, J. Boyce, M. Schieber,

H. Hermon, “High-Resolution Direct-Detection X-ray Imagers,” *Proc. Medical Imaging,* SPIE vol. 3977, pp. 418-428, 2000.

[10] M. Schieber, H. Hermon, A. Zuck, A. Vilensky, L. Melekhov, R. Shatunovsky, E. Meerson, Y. Saado, “Theoretical and Experimental Sensitivity to X-rays of Single Crystal Detectors,” *Nucl. Instr. Meth. Phys. Res. A,* vol. 458, pp. 41-46, 2001.

[11] F. Greuter and G. Blatter, “Electrical Properties of Grain Boundaries in Polycrystalline Compound Semiconductors,” *Semicond. Sci. Tech.,* vol. 5, pp. 111-137, 1990.

[12] K. L. Chopra, *Thin Film Phenomena*, pp. 189-195, McGraw-Hill, New York, 1969.

[13] H. C. Card, and E. S.Yang, “Electronic Processes at Grain Boundaries in Polycrystalline Semiconductor Under Optical Illumination,” *IEEE Trans. Electron Devices,* vol. 24**,** pp. 397- 402, 1977.

[14] H. K. Hecht, “Zum mechanismus des lichtelektrischen primastromers in isolierenden kristallen,” *Z. Phys.,* vol. **77**, pp. 235-243, 1932.

[15] A. Levi, M. Schieber, and Z. Burshtein, “Carrier surface recombination in HgI_2 photon detectors,” *J. Appl. Phys.,* vol. 54, pp. 2472-2476, 1983.

[16] G. Zentai, L. Partain, R. Pavlyuchkova G. Virshup, A. Zuck, L. Melekhov, O. Dagan, A. Vilensky and H.Gilboa, “Large Area Mercuric Iodide X-Ray Imager”, *Proc., SPIE in Medical Imaging 2002: Physics of Medical Imaging , conf. ,* San Diego, February 2002, in press.

[17] A. Levi, A. Burger, J. Nissenbaum, M. Schieber, and Z. Burshtein, “Search for improved surface treatment procedures in fabrication of HgI_2 x-ray spectrometers,” *Nucl. Instr. Meth.,* vol. 213, pp. 35-38, 1983.

* email:- asaf.zuck@realtimeradiography.com; phone: 972-2-653-7655; fax:- 972-2-648-1121

** email:- schieber@vms.huji.ac.il; phone:- 972-2-658-4364; fax:- 972-2-566-3878

*** email:- zeevb@bgumail.bgu.ac.il

Figure captions

Fig. 1. Theoretical voltage-signal versus time traces foe various relations among transit time t_t, trapping time τ, and surface-trapped charge-emission time τ_{em}.

Fig. 2. Schematic illustration of a typical electrical setup for measurement of the transient voltage across a biased HgI_2 sample exposed to high-energy alpha-particle radiation

Fig. 3. Voltage signal versus time traces in a negatively (a) –80V-, or positively (b) +200V biased polycrystalline HgI_2 x-ray detector following absorption of 5.5 MeV alpha particles near the front electrode.

Fig. 4. electron- (a) and hole (b) transit times across the sample of Fig. 3 as functions of 1000/V.

Fig. 5. "Effective" transit time $t_{0.95}$ as a function of 1000/V for electrons (a) and holes (b).

Fig. 6. Charge collection versus time traces for electrons (a) or holes (b), exhibiting delayed emission of charge from near-surface traps.

Fig. 7. Collected charge versus electric field for electrons (a) and holes (b).

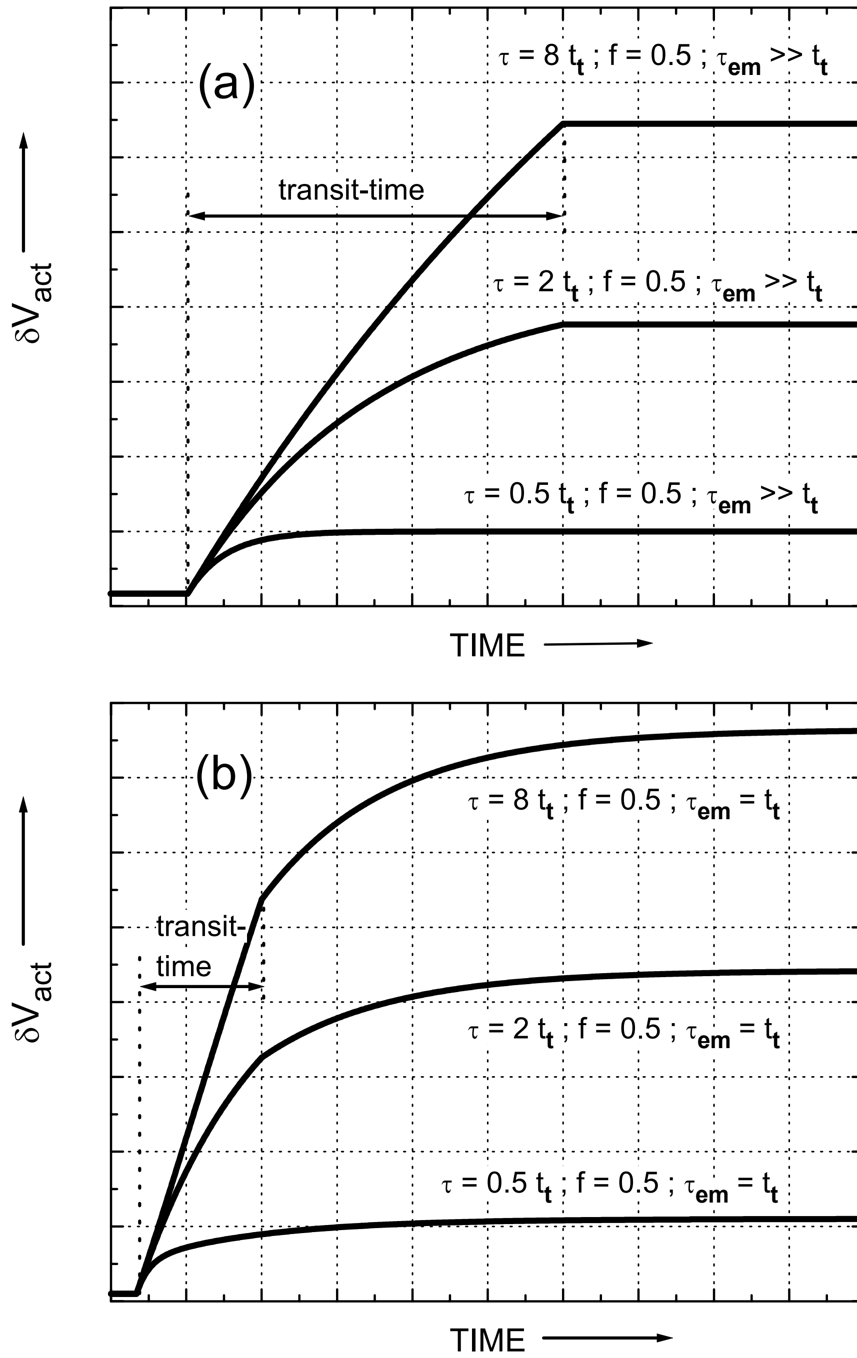

Zuck et al
Fig. 1

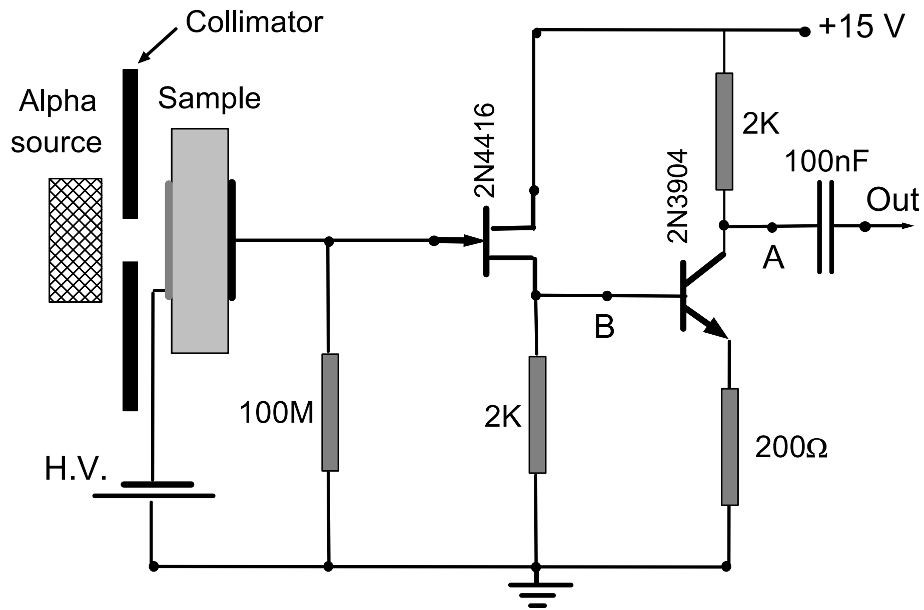

Zuck et al
Fig. 2

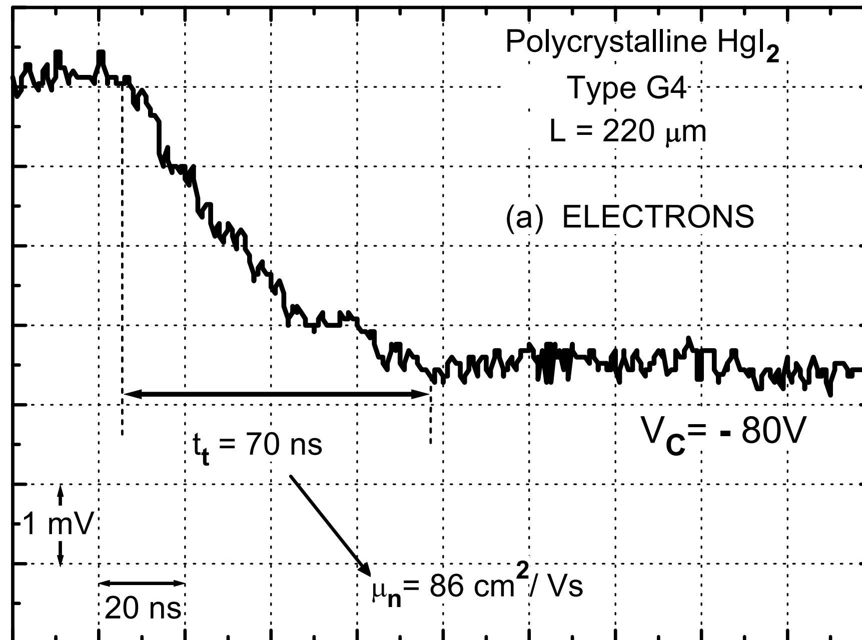

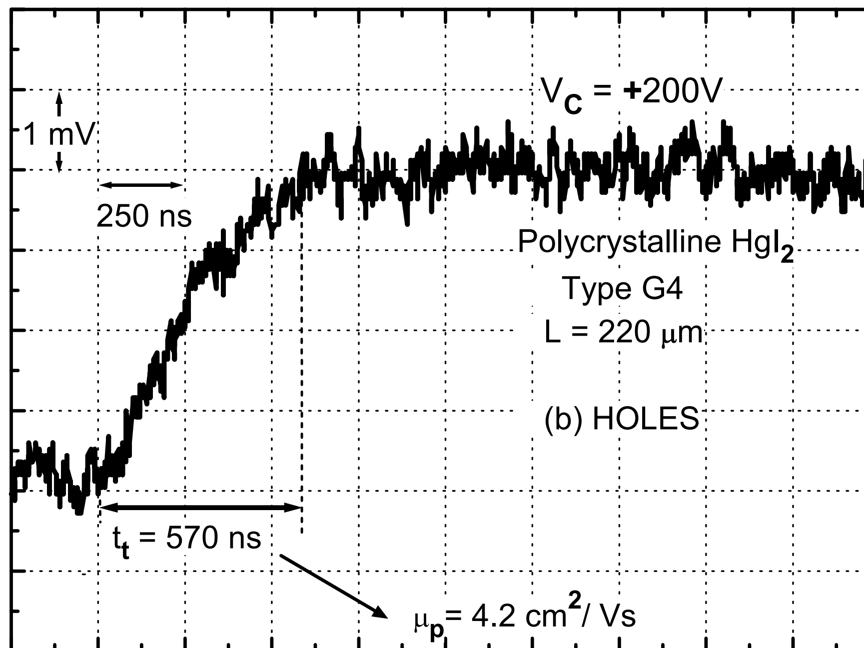

Zuck et al
Fig. 3

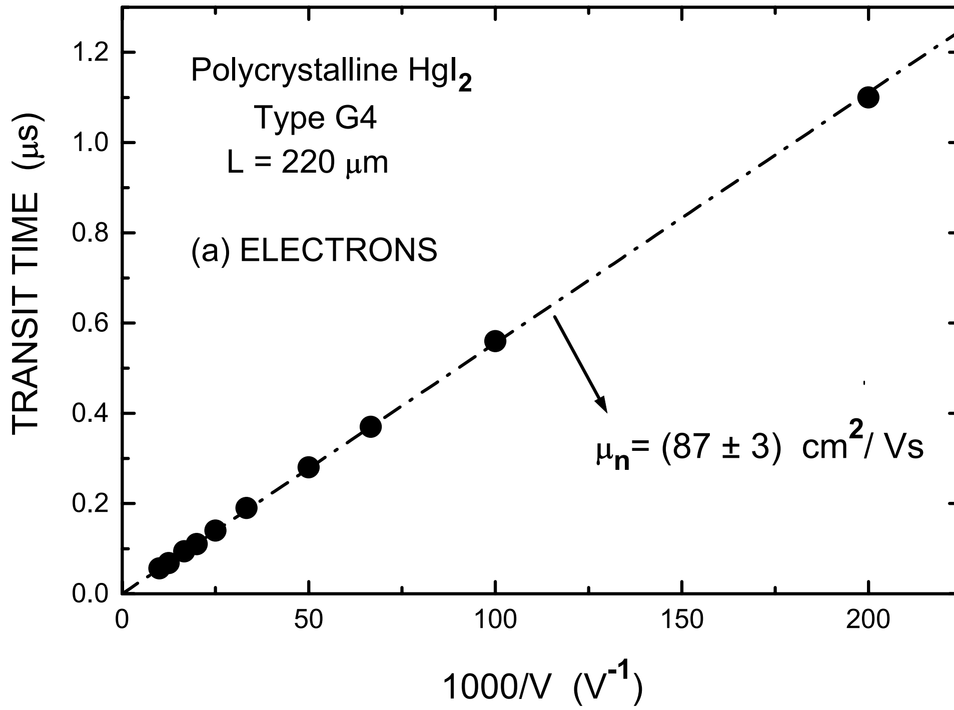

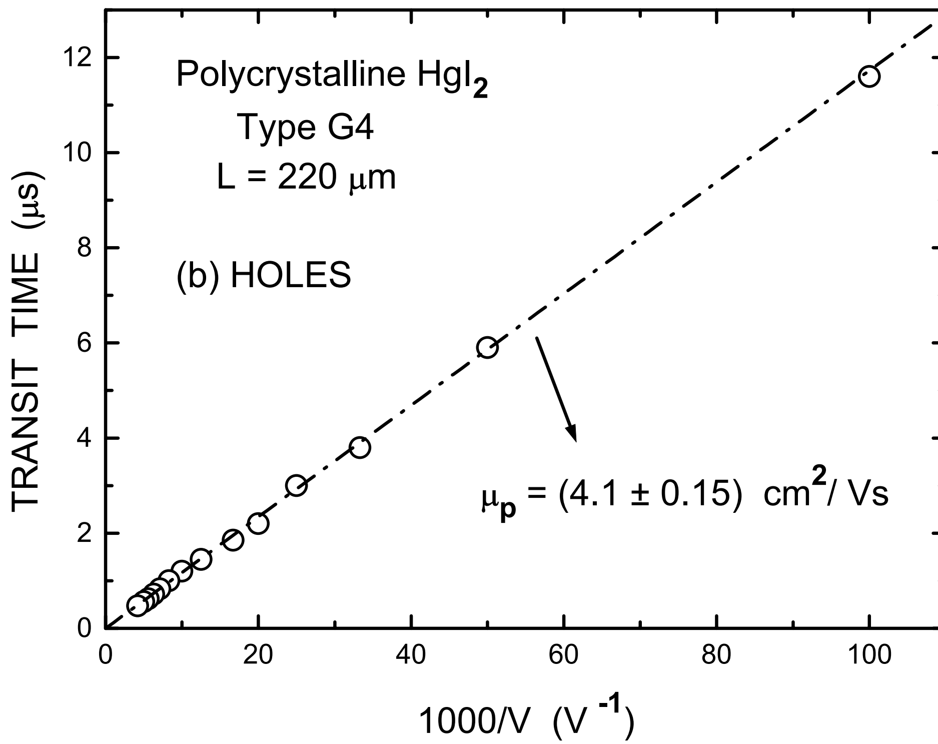

Zuck et al
Fig. 4

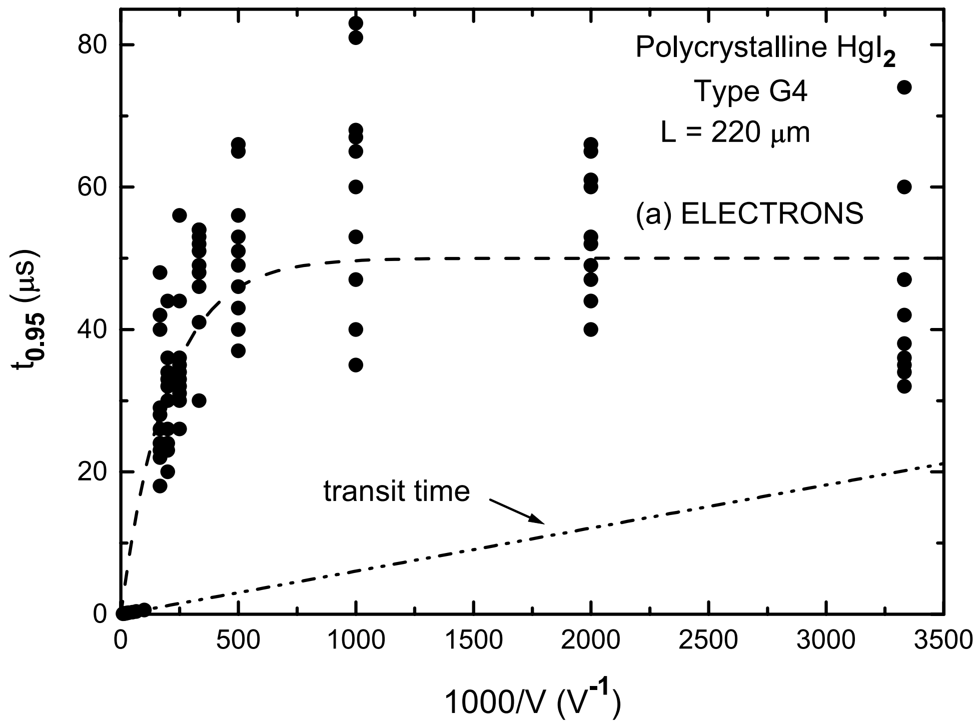

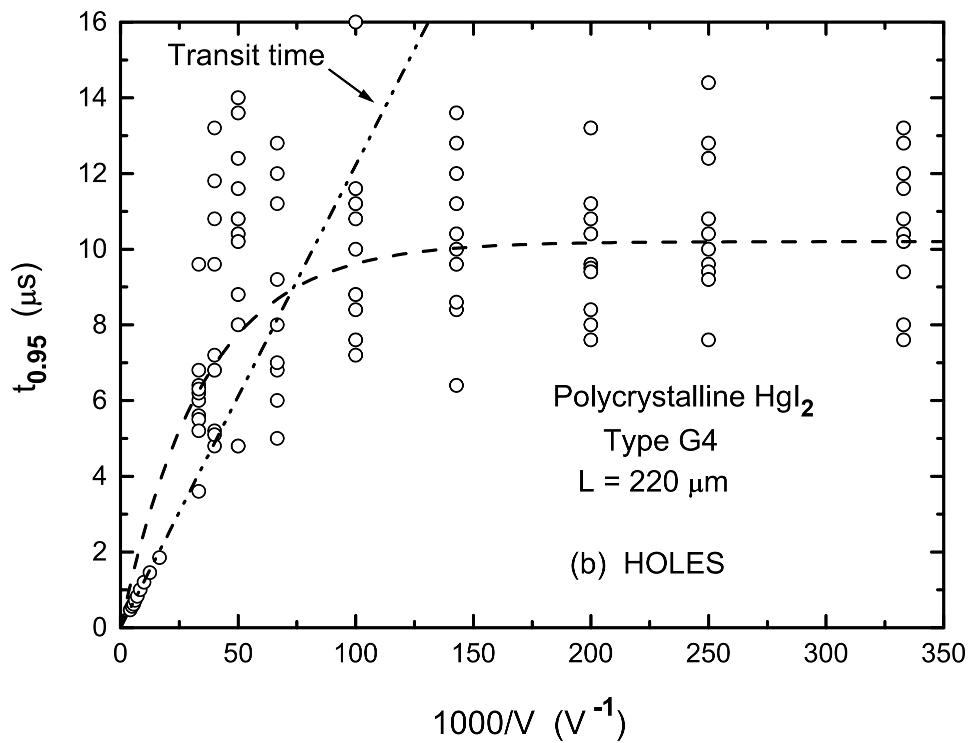

Zuck et al
Fig. 5

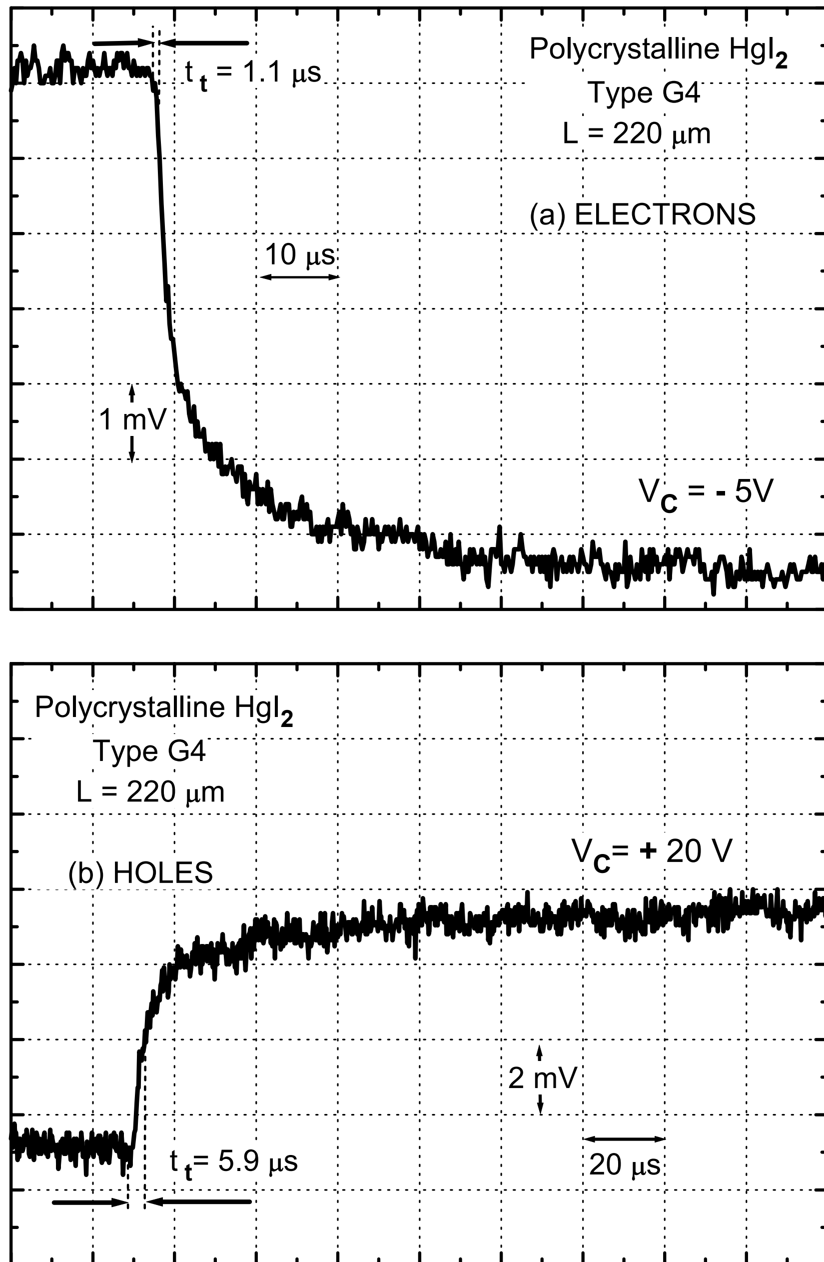

Zuck et al
Fig. 6

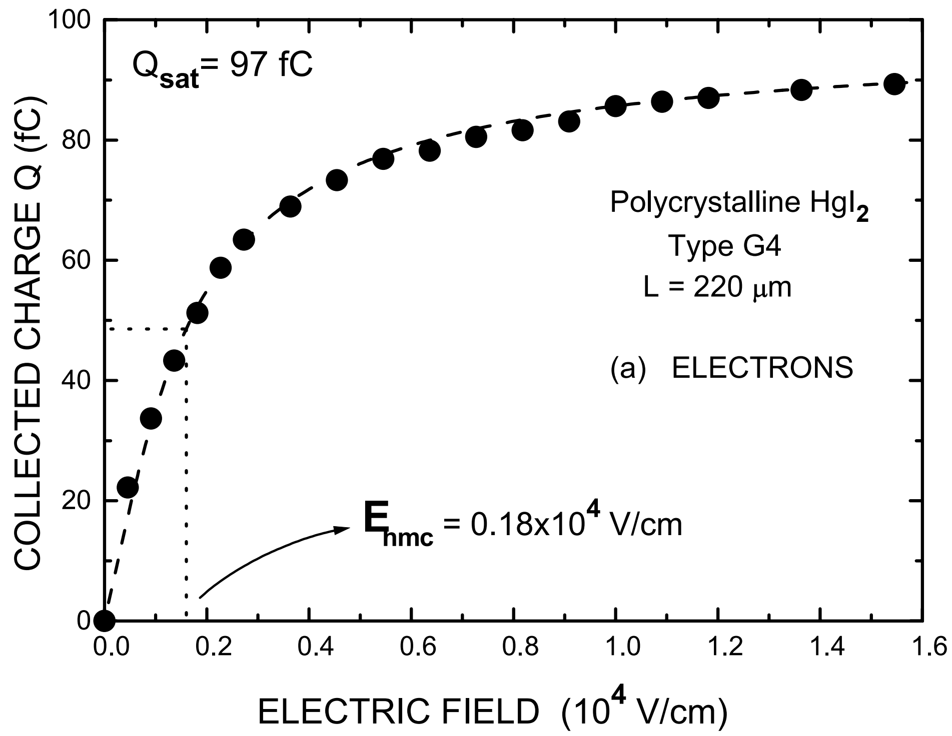

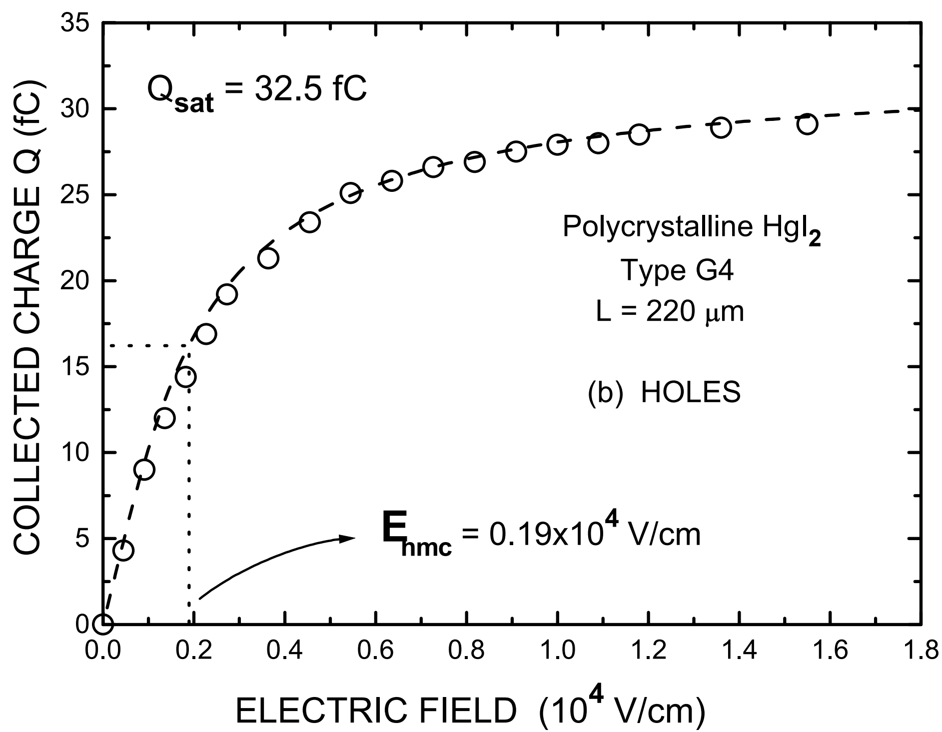

Zuck et al
Fig. 7